Network Neutrality Inference

Zhiyong Zhang[1][2]*, Ovidiu Mara[2], and Katerina Argyraki[2]

[1]UESTC, China
[2] EPFL, Switzerland

ABSTRACT

When can we reason about the neutrality of a network based on external observations? We prove conditions under which it is possible to (a) detect neutrality violations and (b) localize them to specific links, based on external observations. Our insight is that, when we make external observations from different vantage points, these will most likely be inconsistent with each other if the network is not neutral. Where existing tomographic techniques try to form solvable systems of equations to infer network properties, we try to form *un*solvable systems that reveal neutrality violations. We present an algorithm that relies on this idea to identify sets of non-neutral links based on external observations, and we show, through network emulation, that it achieves good accuracy for a variety of network conditions.

Categories and Subject Descriptors

C.2.3 [**Computer Communication Networks**]: Network monitoring

Keywords

Network neutrality; network tomography

1. INTRODUCTION

Once a fundamental Internet property, network neutrality cannot be taken for granted today. There is evidence that Internet service providers (ISPs) differentiate against certain applications, typically BitTorrent [31], by deprioritizing [18], blocking [12], or shaping [11, 16] its traffic. More recently, there is evidence that ISPs are differentiating against traffic originating from specific content providers [1]. We are not saying that such differentiation should be illegal (although it is, in certain countries); our position is that—whether illegal or not—it should be transparent: if an ISP differentiates against specific end-hosts, protocols, or applications, that should be visible to the affected parties and regulators.

In this paper, we address two questions:

(a) Which neutrality violations can be detected based on external observations? There exist proposals for detecting specific kinds of neutrality violation. For instance, several systems can detect whether a network path differentiates based on transport- or application-layer information [18, 31, 15, 11]; however, they cannot detect differentiation based on source or destination IP address, even though end-users suspect that it does occur [1]. To the best of our knowledge, there exists no formal definition of which kinds of neutrality violation are detectable in the first place.

(b) Which neutrality violations can be localized to a specific link or sequence of links and how? Most existing systems can detect whether a *network path* violates neutrality, but they cannot localize it to a specific link or link sequence. An exception is NetPolice, which can determine whether a specific ISP violates neutrality by explicitly measuring the ISP's performance for different traffic flows using traceroute probes [31]. To the best of our knowledge, there exists no system that can localize a neutrality violation to a specific link sequence without explicitly measuring its performance.

Our approach is inspired by network performance tomography, whose goal is to infer performance properties of links (loss rate, latency, congestion status, or congestion probability) based on external observations, i.e., without monitoring these links directly. A tomographic technique typically forms a system of equations

$$\vec{y} = \mathbf{A} \cdot \vec{x},$$

where $\vec{y}$ is a given vector of external observations (end-to-end path measurements), $\mathbf{A}$ is a given matrix that specifies the relationships between links and paths, and $\vec{x}$ is the vector of link properties that we are trying to infer. It then estimates $\vec{x}$, either by solving this system of equations (when it has a unique solution [7, 8, 6, 22, 21, 14]) or by picking a solution that has some desirable property, e.g., assumes the smallest number of problematic links [23, 13, 26, 10] or occurs with the highest probability [22]. This approach fundamentally relies on the assumption that the network is neutral (each link treats traffic from all paths the same), otherwise it would be impossible to express path measurements as a function of link properties and form a solvable system of equations.

Our insight is that, if the network is not neutral, when we make external observations from different vantage points, these will most likely be "inconsistent" with each other, i.e., any system of equations that we form based on them will be unsolvable. So, in a sense, we turn network performance tomography on its head: where existing tomographic techniques assume network neutrality and try to form solvable systems of equations to infer network properties, we try to form *un*solvable systems that reveal neutrality violations. By applying this idea to carefully chosen "slices" of the network, we can reason not only about the neutrality of the entire network, but also that of link sequences or individual links.

One challenge in turning this insight into a practical algorithm is that, in practice, a network link that does not explicitly employ traffic differentiation (hence would be considered "neutral" by existing neutrality definitions) may behave "non-neutrally," e.g., it may appear to be congested to one traffic flow but non-congested to another, over the same time interval. Such network behavior may also lead to inconsistent external observations, and a naïve application of our theory would misinterpret these as willful neutrality violations. We present experimental evidence that we can avoid such

*This work was done at EPFL, when Zhiyong was a visiting PhD student in the Network Architecture Lab.

SIGCOMM'14, August 17–22, 2014, Chicago, IL, USA.

ACM 978-1-4503-2836-4/14/08 ...$15.00.
http://dx.doi.org/10.1145/2619239.2626308.

misleading inconsistencies by comparing observations of similarly sized traffic aggregates.

After describing our terminology and notation (Section 2), we make the following contribution: we prove conditions under which a neutrality violation is "observable," i.e., it manifests as a set of inconsistent external observations (Section 3), and a non-neutral link sequence is "identifiable," i.e., it causes inconsistent external observations that cannot be attributed to any other link sequence (Section 4). We also present an algorithm that takes as input a network graph and external observations, and it identifies all the non-neutral link sequences that are identifiable (Section 5). Finally, we present an initial experimental evaluation of our algorithm on small topologies, based on an open-source network emulator [2], and we show that it achieves good accuracy in a variety of network conditions (Section 6). We close with a discussion of open issues (Section 7), related work (Section 8), and conclusions (Section 9).

2. SETUP

In this section, we present our goal (Section 2.1), assumptions (Section 2.2), and theoretical model (Section 2.3).

2.1 Goal

Our goal is to design an algorithm that takes as input a network graph and external observations (end-to-end measurements), and it identifies non-neutral link sequences. Given that certain neutrality violations are infeasible to detect (Section 3), our algorithm will suffer some false-negatives, but, ideally, it should not suffer false-positives, i.e., a neutral link sequence should never be incorrectly identified as non-neutral.

Neutrality violation is typically informally defined as differentiation based on flow type, i.e., the contents of the IP header, transport-layer header, and/or payload. For example, a network link may throttle traffic coming from a specific content provider (based on IP addresses) or from a specific peer-to-peer (P2P) network (based on port numbers or deep-packet inspection). When a network link throttles a traffic flow, it upper-bounds the rate at which the flow can send traffic, typically below the rate at which the flow generates traffic; this results in a higher packet-loss rate and/or latency than the one experienced by unthrottled traffic. So, traffic differentiation results in different traffic flows experiencing different performance when traversing the same link(s).

We define "neutrality violation" as the situation where traffic from two different network paths experiences different performance when traversing the same network link (formal definition in Section 2.3). Hence, in our model, a flow type is represented by a set of paths. For example, suppose a network link throttles traffic coming from a specific content provider; we model this by saying that the network has two "performance classes," one class comprising all the paths that start at the content provider, and the other class comprising all the other paths. Similarly, suppose a network link throttles a specific kind of P2P traffic; again, we model this by saying that the network has two performance classes, one class comprising all the paths that carry this form of P2P traffic, and the other class comprising all the other paths. We will discuss the reason behind our choice of definition later in the paper, once we have presented our model and results.

We do not assume any knowledge on the network's differentiation criteria, the number of performance classes it distinguishes, or which network paths belong to the same class. If one does have such knowledge, it is possible to detect and localize neutrality violations with a simpler approach than ours. For example, suppose two parties connected to the same ISP suspect that the ISP throttles their P2P traffic; to test this, they can exchange first P2P traffic, then some other kind of traffic, and compare the achieved performance. On the other hand, this approach does not work when (a) the ISP throttles all traffic between the two parties and/or (b) the two parties communicate over more than one ISPs (in general, administrative domains), and any one of them could be throttling their traffic.

2.2 Assumptions

We make three assumptions:

1. We assume the existence of a measurement platform and knowledge of the network graph that interconnects the measurement points. A link in the network graph may correspond to an IP-level link, a domain-level link, or, in general, a sequence of consecutive physical links.

2. We assume that the status of each network link is independent from the status of any other network link.

3. Theorem 1 (Section 3.3) and Lemma 3 (Section 4.2) assume that: within any given time interval, if a non-neutral network link introduces non-negligible packet loss in its top-priority performance class (formal definition in Section 2.3), it introduces non-negligible packet loss in the other performance classes as well.

Assumptions #2 and #3 simplify our analysis and algorithm, but they are not fundamental to our approach; we discuss how we plan to relax them in our technical report [32].

2.3 Model

Links and paths.

We represent the network as a tuple $G = (V, L, P)$. V and L are, respectively, the nodes and links (edges) of the network graph. We distinguish two kinds of nodes: *end-hosts* and *relays* (the latter correspond to intermediate elements like switches or routers). A *path* is a loop-free sequence of consecutive links starting and ending at end-hosts, and P is the set of all the paths in the network that are currently used.

We use l to refer to some link in L, and l_k to refer to the k-th link assuming an arbitrary ordering of all the $|L|$ links. We use λ to refer to a loop-free sequence of consecutive links in L. We use p to refer to some path in P, and p_i to refer to the i-th path assuming an arbitrary ordering of all the $|P|$ paths.

A *pathset* is a set of paths, and we denote the set of all pathsets in the network with P^* (the power set of P). We use π to refer to some pathset. Given a set of pathsets Π, we use π_i to refer to the i-th pathset assuming an arbitrary ordering of all the pathsets in Π.

We define the following helper functions: $Paths(l)$ is the set of all paths that traverse link l, $Paths(\lambda)$ is the set of all paths that traverse all the links in link sequence λ, $Links(p)$ is the set of all links traversed by path p, and $Links(\pi)$ is the set of all links traversed by at least one path in pathset π.

We say that link l is *distinguishable* from link l', when $Paths(l) \neq Paths(l')$.

Performance classes and numbers.

A *performance class* is a set of paths (that, as we will see below, are treated the "same" by the network), and we denote the set of all performance classes by C. We use c_n to refer to the n-th class assuming an arbitrary ordering of all the $|C|$ classes.

A link is characterized by a set of performance numbers $\{x(n) \mid n = 1..|C|\}$. When traffic from a path that belongs to the n-th class traverses this link, it experiences performance $x(n)$. We use

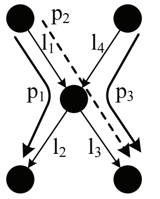

(a) Network graph G.

	l_1	l_2	l_3	l_4
$\{p_1\}$	1	1	0	0
$\{p_2\}$	1	0	1	0
$\{p_3\}$	0	0	1	1
$\{p_1, p_2\}$	1	1	1	0
$\{p_1, p_3\}$	1	1	1	1
$\{p_2, p_3\}$	1	0	1	1
$\{p_1, p_2, p_3\}$	1	1	1	1

(b) A routing matrix $\mathbf{A}$.

Figure 1: Example network with links $L = \{l_1, l_2, l_3, l_4\}$, paths $P = \{p_1, p_2, p_3\}$, and performance classes $C = \{\{p_1, p_3\}, \{p_2\}\}$. Link l_1 is non-neutral: it treats traffic from path p_2 worse than traffic from path p_1.

$\{x_k(n) \mid n = 1..|C|\}$ to particularly denote the performance numbers of link l_k.

We say that a link is *neutral* when its performance number is the same for all performance classes: $x(n) = x,\ \forall n = 1..|C|$; otherwise, we say that the link is *non-neutral*. When there is only one performance class in the network, by definition, all links are neutral. We use x_k to particularly denote the performance number of neutral link l_k. We denote all the neutral links in the network by L_n, and all the non-neutral links in the network by $L_{\bar{n}}$. The *top-priority class* of a non-neutral link is the class for which the link has the highest performance.

For example, in Figure 1(a), there are two performance classes, $\{p_1, p_3\}$ and $\{p_2\}$. Non-neutral link l_1 has performance numbers $\{x_1(1), x_1(2)\}$, while neutral link l_3 has performance number x_3. Traffic traversing l_1 experiences different performance, depending on which path it belongs to: traffic from path p_1 experiences performance $x_1(1)$, whereas traffic from path p_2 experiences performance $x_1(2)$. In contrast, all traffic traversing link l_3 experiences the same performance x_3.

Similarly, a link sequence is characterized by a set of performance numbers $\{\hat{x}(n) \mid n = 1..|C|\}$.

Finally, a pathset π is characterized by a performance number y. Given a set of pathsets Π, we use y_i to denote the performance number of pathset π_i.

Performance metrics.

In our experimental evaluation, we use the performance metric introduced in [22], which is defined as follows:

▷ Time is divided into intervals.

▷ We say that a link, link sequence, or path is *congestion-free* during a given time interval, when it introduces (or experiences, in the case of a path) negligible packet loss during that interval.

▷ The performance numbers of a link or link sequence λ are $\{\hat{x}(n) \equiv \log(\mathbb{P}(\lambda, c_n)) \mid n = 1..|C|\}$, where $\mathbb{P}(\lambda, c_n)$ is the probability that λ is congestion-free with respect to performance class c_n during any given time interval.

▷ The performance number of pathset π is $y \equiv \log(\mathbb{P}(\pi))$, where $\mathbb{P}(\pi)$ is the probability that all the paths in π are congestion-free during any given time interval.

In general, we can use any metric that is "additive" in the following sense:

1. The performance of a link sequence λ for class c_n is equal to the sum of the performance of its member links for that class:

$$\hat{x}(n) = \sum_{k \mid l_k \in \lambda} x_k(n). \tag{1}$$

   For example, in Figure 1(a), link sequence $\langle l_1, l_3 \rangle$ has performance numbers $\{\hat{x}(1) = x_1(1) + x_3, \hat{x}(2) = x_1(2) + x_3\}$.

2. In a neutral network, the performance of a pathset π is equal to the sum of the performance of its member links:

$$y = \sum_{k \mid l_k \in Links(\pi)} x_k. \tag{2}$$

   For example, if the network in Figure 1(a) was neutral, pathset $\{p_1, p_2\}$ would have performance number $y = x_1 + x_2 + x_3$.

We restrict ourselves to performance metrics that satisfy both Equations 1 and 2, because we have found that these reveal the largest number of neutrality violations. Not all intuitive metrics fall into this category; we discuss how to address this limitation in Section 7.

Definition of network neutrality.

A *neutral link sequence* is a sequence of neutral links and a *neutral network* is one that has only neutral links. Conversely, a *non-neutral* sequence or network is one that includes at least one non-neutral link.

Neutrality inference.

The input to our problem consists of: the network G and the performance number of any pathset $\pi \in P^*$. The desired output is the set of non-neutral links $L_{\bar{n}}$.

Generalized routing matrix.

A *generalized routing matrix* represents the relationships between the links L and a set of pathsets Π (Figure 1(b)). More formally: Given a set of pathsets Π, a generalized routing matrix $\mathbf{A}(\Pi)$ is a $|\Pi| \times |L|$ matrix with

$$\mathbf{A}_{ik} = \begin{cases} 1, & \text{if at least one path in pathset } \pi_i \\ & \text{traverses link } l_k \\ 0, & \text{otherwise.} \end{cases}$$

Systems of equations for a neutral network.

Here are some of the equations we could write for the network in Figure 1, if it was neutral:

$$\begin{aligned} \{p_1\}: &\quad y_1 = x_1 + x_2 \\ \{p_2\}: &\quad y_2 = x_1 + x_3 \\ \{p_1, p_2\}: &\quad y_3 = x_1 + x_2 + x_3. \end{aligned}$$

Any such system of equations can be summarized as

$$\vec{y} = \mathbf{A}(\Pi) \cdot \vec{x}, \tag{3}$$

where $\vec{x} = \{x_k \mid k = 1..|L|\}$ and $\vec{y} = \{y_i \mid i = 1..|\Pi|\}$.

When the network is not neutral, the equations in System 3 are incorrect and—as we will see—the system is often unsolvable. This observation is the cornerstone of our work.

3. NETWORK NON-NEUTRALITY

In this section, we present a condition on the network G and the location of the non-neutral links $L_{\bar{n}}$, which is necessary and sufficient for observing non-neutrality using our approach. When a non-neutral network meets this condition, we can observe that it is non-neutral; when it does not meet this condition, it appears neutral to our approach. We first define "observability" (Section 3.1) and the "equivalent neutral network," the basic construct that we use to formulate our result (Section 3.2), then state the condition and illustrate with examples (Section 3.3). The proof of the theorem is in our technical report [32].

3.1 Definition of Observability

LEMMA 1. *Consider a network with paths P. If there exists a set of pathsets $\Pi \subseteq P^*$ such that System 3 does not have a solution, then the network is non-neutral.*

The proof is trivial: When all the links are neutral, the routing matrix correctly captures the relationships between the link performance numbers $\vec{x} = \{x_k \mid k = 1..|L|\}$ and the external observations $\vec{y}$, so System 3 has at least one solution.

Lemma 1 says that, if System 3 has no solution, the only possible explanation is that the network is non-neutral. For example, consider the network shown in Figure 1 and the system of equations

$$\begin{aligned} \{p_1\}: &\qquad y_1 = x_1 + x_2 \\ \{p_2\}: &\qquad y_2 = x_1 + x_3 \\ \{p_3\}: &\qquad y_3 = x_3 + x_4. \end{aligned}$$

Suppose we observe that (a) $y_1 = y_3 = 0$ (paths p_1 and p_3 are always congestion-free), whereas (b) $y_2 \neq 0$ (path p_2 is occasionally congested). These two observations are inconsistent: (a) indicates that $x_k = 0$ for all k (all the links are always congestion-free), whereas (b) indicates that either $x_1 \neq 0$ or $x_3 \neq 0$ (either l_1 or l_3 is occasionally congested). The only possible explanation for this inconsistency is that l_1 and/or l_3 are non-neutral and treat traffic from path p_2 worse than the other traffic.

DEFINITION 1. *Consider a non-neutral network with paths P. We say that the network's neutrality violation is* observable*, when there exists a set of pathsets $\Pi \subseteq P^*$ such that System 3 does not have a solution.*

There exist neutrality violations that are not observable with our approach. For example, consider the network shown in Figure 2(a), where link l_1 is non-neutral, treating traffic from path p_2 worse than traffic from path p_1. In this particular network, there exists no unsolvable System 3. The intuition is that the worse treatment that l_1 inflicts on path p_2 can always be attributed to link l_3. As a result, any set of external observations can be explained through a neutral behavior of the links, which means that we cannot detect neutrality violation based on external observations.

3.2 Equivalent Neutral Network

From the point of view of the end-hosts, any non-neutral network with $|L_n|$ neutral links, $|L_{\bar{n}}|$ non-neutral links, and $|C|$ performance classes is equivalent to a neutral network with $|L_n| + |L_{\bar{n}}| \cdot |C|$ (neutral) links; by "equivalent" we mean that the two networks produce the same external observations. To generate an *equivalent neutral network*, we map each original non-neutral link l into $|C|$ *virtual* neutral links, one of them modeling l's common queue and the rest of them modeling l's regulation of the lower-priority classes.

Figure 2 shows an example: in the original network, non-neutral link l_1 has performance numbers $x_1(1)$ and $x_1(2)$; in the neutral equivalent, l_1 is mapped to two virtual links:

a) Virtual link $l_1^+(1)$ models l_1's common queue. It has performance number $x_1(1)$, and it is traversed by both paths. It captures any bad performance that link l_1 may inflict on p_1, which will necessarily also be inflicted on p_2 (since it is lower-priority).

b) Virtual link $l_1^+(2)$ models l_1's regulation of performance class c_2. It has performance number $x_1(2) - x_1(1)$, and it is traversed only by path p_2. It captures any extra bad performance that link l_1 may inflict on p_2 due its regulation of performance class c_2.

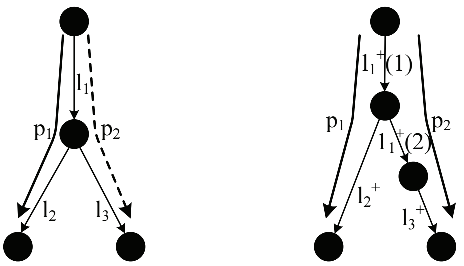

(a) Original network G. (b) Neutral equivalent G^+.

	l_1	l_2	l_3
$\{p_1\}$	1	1	0
$\{p_2\}$	1	0	1

(c) A routing matrix $\mathbf{A}$.

	$l_1^+(1)$	$l_1^+(2)$	l_2^+	l_3^+
$\{p_1\}$	1	0	1	0
$\{p_2\}$	1	1	0	1

(d) A routing matrix $\mathbf{A}^+$.

Figure 2: A non-neutral network (and its neutral equivalent) where neutrality violation is non-observable. There are two performance classes $C = \{\{p_1\}, \{p_2\}\}$. Link l_1 is non-neutral: it treats traffic from p_2 worse than traffic from p_1.

An original non-neutral network $G = (V, L, P)$ and a neutral equivalent $G^+ = (V^+, L^+, P)$ are related as follows:

a) For each neutral link $l \in L_n$ with performance number x, there exists a link $l^+ \in L^+$ with the same performance number x and $Paths(l^+) = Paths(l)$.

b) For each non-neutral link $l \in L_{\bar{n}}$ with performance numbers $\{x(n) \mid n = 1..|C|\}$ and top-priority class c_{n^*}, there exist $|C|$ links $\left\{l^+(n) \mid n = 1..|C|\right\} \in L^+$, where:

   i) $l^+(n^*)$ has performance number $x(n^*)$ and $Paths(l^+(n^*)) = Paths(l)$.

   ii) $l^+(n), \forall n \neq n^*$ has performance number $x(n) - x(n^*)$ and $Paths(l^+(n)) = Paths(l) \cap c_n$.

As a second example, Figure 3(a) shows the neutral equivalent for the network in Figure 1(a): neutral link l_2 is mapped to virtual link l_2^+, while non-neutral link l_1 is mapped to $l_1^+(1)$ and $l_1^+(2)$.

For any non-neutral network, there exists at least one neutral equivalent and potentially more. A neutral equivalent may include "loop links," which start and end at the same node; we show examples in our technical report. We use $\mathbf{A}^+$ to denote a generalized routing matrix of an equivalent neutral network.

3.3 Condition for Observability

THEOREM 1. *Consider a non-neutral network with links L, and its equivalent neutral network with links L^+. The network's neutrality violation is observable, if and only if there exists at least one virtual link $l^+(n) \in L^+$ that is distinguishable from any link in L.*

We illustrate with three examples:

Non-observable violation.

Consider again the non-neutral network in Figure 2(a) and its neutral equivalent in Figure 2(b). In this case, none of the two virtual links in the neutral equivalent satisfies the condition in Theorem 1: $l_1^+(1)$ is indistinguishable from l_1, and $l_1^+(2)$ is indistinguishable from l_3. Therefore, according to the theorem, this neutrality violation is not observable. Indeed, we said earlier that l_1's worse effect on p_2 can always be attributed to l_3 (Section 3.1). This is an informal way of saying that $l_1^+(2)$ is indistinguishable from

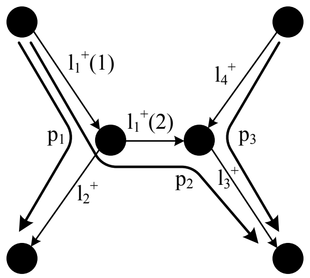

(a) Neutral equivalent G^+.

	$l_1^+(1)$	$l_1^+(2)$	l_2^+	l_3^+	l_4^+
$\{p_1\}$	1	0	1	0	0
$\{p_2\}$	1	1	0	1	0
$\{p_3\}$	0	0	0	1	1
$\{p_1, p_2\}$	1	1	1	1	0
$\{p_1, p_3\}$	1	0	1	1	1
$\{p_2, p_3\}$	1	1	0	1	1
$\{p_1, p_2, p_3\}$	1	1	1	1	1

(b) A routing matrix $\mathbf{A}^+$.

Figure 3: Neutral equivalent for the network shown in Figure 1.

l_3. Theorem 1 expresses this insight: if a virtual link $l^+(n)$ in the neutral equivalent is indistinguishable from some other link l' in the original network, then the non-neutral behavior captured by $l^+(n)$ can be masked, because its effect can always be attributed to l'.

Observable violation #1.

Consider again the non-neutral network in Figure 1(a) and its neutral equivalent in Figure 3(a). In this case, virtual link $l_1^+(2)$ is distinguishable from any link in L. Therefore, according to the theorem, this neutrality violation is observable. Indeed, we said earlier that l_1's effect on p_2 cannot be attributed to any set of neutral links (Section 3.1). Theorem 1 expresses this insight: if a virtual link $l^+(n)$ in the neutral equivalent is distinguishable from any link in the original network, then the non-neutral behavior captured by $l^+(n)$ cannot be masked, because it cannot be attributed to any other link(s).

Observable violation #2.

Consider the non-neutral network in Figure 4(a) and its neutral equivalent in Figure 4(b). Link l_1 introduces congestion into class-2 traffic with probability 0.5, while the rest of the network is congestion-free. In this case, virtual link $l_1^+(2)$ is distinguishable from any link in L. Therefore, according to the theorem, this neutrality violation is observable.

At first, it may seem counter-intuitive that this neutrality violation is observable, as it looks similar to the one in Figure 2 (which is not). However, a closer look reveals that, in this case, there does exist an unsolvable system of equations:

$$\begin{aligned}
\{p_1\}: &\quad y_1 = x_1 + x_2 \\
\{p_2\}: &\quad y_2 = x_1 + x_3 \\
\{p_3\}: &\quad y_3 = x_1 + x_4 \\
\{p_2, p_3\}: &\quad y_4 = x_1 + x_3 + x_4.
\end{aligned}$$

If we monitor this network, we observe that:

$$\begin{array}{ll}
y_1 = 0 & p_1 \text{ is always congestion-free.} \\
y_2 = \log(0.5) & p_2 \text{ is congestion-free w.p. } 0.5. \\
y_3 = \log(0.5) & p_3 \text{ is congestion-free w.p. } 0.5. \\
y_4 = \log(0.5) & \{p_2, p_3\} \text{ is congestion-free w.p. } 0.5.
\end{array}$$

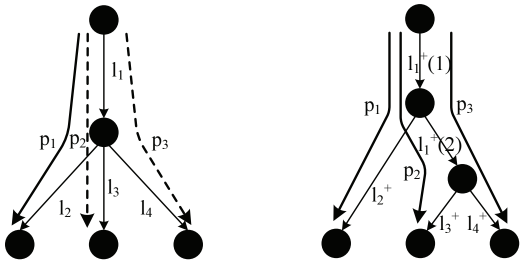

(a) Original network G.
(b) Neutral equivalent G^+.

Figure 4: A non-neutral network where neutrality violation is observable. There are two performance classes $C = \{\{p_1\}, \{p_2, p_3\}\}$. Link l_1 has performance numbers $\{x_1(1) = 0, x_1(2) = \log(0.5)\}$. The other links have performance numbers $x_2 = x_3 = x_4 = 0$.

These observations are inconsistent: (a) y_1 indicates that $x_1 = x_2 = 0$, which means that link l_1 is always congestion-free. (b) $\{y_2, y_3, y_4\}$ form a system with unique solution:

$$\begin{array}{ll}
x_1 = \log(0.5) & l_1 \text{ is congestion-free w.p. } 0.5. \\
x_3 = 0 & l_3 \text{ is always congestion-free.} \\
x_4 = 0 & l_4 \text{ is always congestion-free.}
\end{array}$$

So, if we observe only path p_1, we conclude that link l_1 is always congestion-free, whereas if we observe only paths $\{p_2, p_3\}$, their congestion can only be attributed to link l_1. The only explanation is that link l_1 is non-neutral and treats traffic from paths $\{p_2, p_3\}$ worse than the rest.

As a side-note, this example illustrates the benefit of using performance metrics that can be defined and measured for pathsets, not only individual paths: The clue that gives away l_1's non-neutrality is the fact that p_2 and p_3 always experience congestion *at the same time*; assuming that link statuses are independent (Section 2.2), this correlation can only be attributed to non-neutral behavior by l_1. This clue emerges only if we observe p_2 and p_3 as a pair and measure the probability that they are both congestion-free. Theorem 1 guarantees that, as long as there exists a distinguishable link $l^+(n)$ in the neutral equivalent, we can form an unsolvable system of equations; this system, however, may include equations on pathsets with more than one path, and we must be able to define and measure their performance.

4. LINK NON-NEUTRALITY

In this section, we present a condition on the paths $Paths(\lambda)$ that traverse a link sequence λ, which is sufficient for correctly inferring λ's neutrality. We first define the "network slice," the basic construct that we use to formulate our result (Section 4.1), then state the condition and illustrate with examples (Section 4.2). The proofs of the lemmas are in our technical report [32].

4.1 Network Slice

Lemma 1 can help us reason not only about the neutrality of the entire network, but also about the neutrality of link sequences, even individual links. For example, consider the network shown in Figure 4(a), where the only link traversed by multiple paths is l_1. If we determine that this network is non-neutral, then the only possible explanation is that link l_1 is non-neutral, as it is the only link that handles traffic from multiple paths and can differentiate between them.

To reason about the neutrality of a link sequence λ, we apply Lemma 1 to a *network slice* G_λ, chosen such that any observable neutrality violation of this slice can only be attributed to λ. More specifically, we form a specialized version of System 3:

$$\vec{y} = \mathbf{A}_\lambda(\Pi_\lambda) \cdot \vec{x}. \qquad (4)$$

We specify how we form this system in our technical report; here, we only illustrate by example.

To reason about the neutrality of link l_1 in Figure 5(a), we form System 4 for $\lambda = \langle l_1 \rangle$ as follows:

a) We create a special set of pathsets $\Pi_{\langle l_1 \rangle}$ as follows:

   i) We identify all path pairs whose only shared link is l_1: $\{p_1, p_4\}$, $\{p_2, p_4\}$, and $\{p_3, p_4\}$.

   ii) $\Pi_{\langle l_1 \rangle}$ consists of these path pairs plus their individual paths: $\Pi_{\langle l_1 \rangle} = \{\{p_1\}, \{p_2\}, \{p_3\}, \{p_4\}, \{p_1, p_4\}, \{p_2, p_4\}, \{p_3, p_4\}\}$.

b) We create network slice $G_{\langle l_1 \rangle}$ by abstracting away all individual links in the network other than l_1, as shown in Figure 5(b).

c) We form the system of equations that corresponds to generalized routing matrix $\mathbf{A}_{\langle l_1 \rangle}(\Pi_{\langle l_1 \rangle})$, shown in Figure 5(c).

There are two key points about System 4: First, it typically consists of a small number of equations, because Π_λ tends to be small (for any link sequence λ, there are typically few path pairs whose *only* common link sequence is λ). Second, once we have created Π_λ, the topology of the overall network becomes irrelevant; the only factors that play a role in System 4 are the performance numbers of the paths and path pairs in Π_λ. This is different from existing tomography techniques, which typically combine large numbers of path measurements into a single large system of equations that is determined by the topology of the entire network.

4.2 Identifiability of Non-neutral Links

LEMMA 2. *Consider a link sequence λ and its set of pathsets Π_λ. If System 4 does not have a solution, then λ is non-neutral.*

System 4 is a special version of System 3 where the equations are picked for their particular relationship to link sequence λ. If System 4 does not have a solution, we already know from Lemma 1 that the network slice G_λ is non-neutral; Lemma 2 tells us that link sequence λ in particular is non-neutral. For example, if the system in Figure 5(c) does not have a solution, the only possible explanation is that link l_1 is not neutral. The intuition is related to our discussion on Observable Violation #2 in Section 3.3: pathsets $\{p_1\}, \{p_4\}, \{p_1, p_4\}$ will yield one estimate for l_1's performance; pathsets $\{p_2\}$, $\{p_4\}$, $\{p_2, p_4\}$ will yield a second estimate; these can only be different (and the system in Figure 5(c) unsolvable), if link l_1 treats a subset of the involved paths differently.

DEFINITION 2. *Consider a non-neutral link sequence λ and its set of pathsets Π_λ. We say that λ is* identifiable*, when System 4 does not have a solution.*

There exist non-neutral links that are non-identifiable. For example, suppose we want to reason about the neutrality of link l_2 in Figure 5(a). To create $\Pi_{\langle l_2 \rangle}$, we first identify every path pair whose only shared link is l_2. There are no such path pairs, $\Pi_{\langle l_2 \rangle} = \emptyset$, and we cannot form System 4 for $\lambda = \langle l_2 \rangle$.

LEMMA 3. *Consider a non-neutral link sequence λ with performance numbers $\{\hat{x}(n) \mid n = 1..|C|\}$ and top-priority class c_{n^*}. If the following conditions hold:*

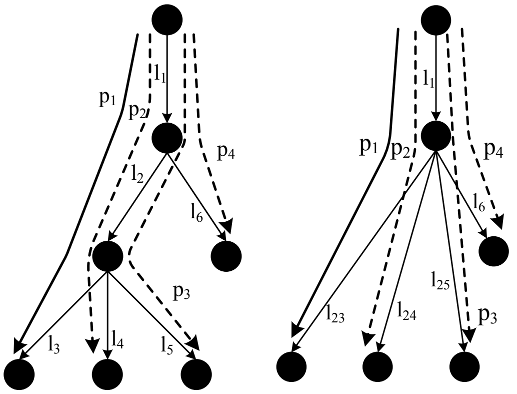

(a) Original network G. (b) Network slice $G_{\langle l_1 \rangle}$.

$$\begin{array}{lll}
\{p_1\}: & y_1 & = x_1 + x_{23} \\
\{p_2\}: & y_2 & = x_1 + x_{24} \\
\{p_3\}: & y_3 & = x_1 + x_{25} \\
\{p_4\}: & y_4 & = x_1 + x_6 \\
\{p_1, p_4\}: & y_5 & = x_1 + x_{23} + x_6 \\
\{p_2, p_4\}: & y_6 & = x_1 + x_{24} + x_6 \\
\{p_3, p_4\}: & y_7 & = x_1 + x_{25} + x_6.
\end{array}$$

(c) System 4 for $\lambda = \langle l_1 \rangle$.

Figure 5: A non-neutral network where neutrality violation is observable. There are two performance classes $C = \{\{p_1\}, \{p_2, p_3, p_4\}\}$, where $\{p_1\}$ has top-priority. Link l_1 is non-neutral, identifiable. Link l_2 is non-neutral, non-identifiable.

- *there exist at least two path pairs π_i, π_j in Π_λ*

$$(\exists\, \pi_i, \pi_j \in \Pi_\lambda);$$

- *and a lower-priority class c_n $(\exists c_{n \neq n^*} \in C)$;*
- *such that π_i is entirely in class c_n and π_j is not*

$$(\pi_i \subset c_n,\ \pi_j \not\subset c_n);$$

then λ is identifiable.

Informally, Lemma 3 says that a non-neutral link sequence is identifiable as long as it is traversed by a sufficiently diverse set of paths: We can determine that link sequence λ is non-neutral, when it causes different path pairs in Π_λ to experience inconsistent performance. This is guaranteed to happen for l_1 in Figure 5(a): on the one hand, path pair $\{p_2, p_4\}$ is entirely in performance class c_2, hence it will yield an estimate of l_1's performance from the point of view of this performance class; on the other hand, path pair $\{p_1, p_4\}$ includes at least one path from performance class c_1, hence it will yield a different estimate of l_1's performance. In contrast, there exist no path pairs at all that share only link l_2 in the same figure, hence we cannot identify it as a non-neutral link.

5. ALGORITHM

We will now present an algorithm that takes as input the network G and the performance number of any pathset π, and it outputs a set of non-neutral link sequences $\Lambda_{\bar{n}}$. We will use three metrics to characterize the quality of the algorithm:

False-negative rate: It is the fraction of non-neutral links that do not participate in any link sequence present in $\Lambda_{\bar{n}}$. E.g., false-negative rate 10% means that 10% of the non-neutral links do not participate in any link sequence present in $\Lambda_{\bar{n}}$.

Algorithm 1 Identification of non-neutral link sequences

```
Input:   The links $L$ and paths $P$
Output:  The set of identif. non-neutral link seqs $\Lambda_{\bar{n}}$

 1: $\Lambda_n \leftarrow \emptyset, \Lambda_{\bar{n}} \leftarrow \emptyset$
 2: for each path pair $\{p_i, p_j\} \in P^*$ do
 3:     $\lambda = Links(p_i) \cap Links(p_j)$
 4:     if $\lambda \notin \Lambda_n$ then
 5:         $\Lambda_n \leftarrow \Lambda_n \cup \{\lambda\},\ \Pi_\lambda \leftarrow \emptyset$
 6:     end if
 7:     $\Pi_\lambda \leftarrow \Pi_\lambda \cup \{\{p_i\}, \{p_j\}, \{p_i, p_j\}\}$
 8: end for
 9: for each link sequence $\lambda \in \Lambda_n$ do
10:     if $|\Pi_\lambda| < 5$ then
11:         $\Lambda_n \leftarrow \Lambda_n \setminus \{\lambda\}$
12:     end if
13:     if system $\vec{y} = \mathbf{A}_\lambda(\Pi_\lambda) \cdot \vec{x}$ has no solution then
14:         $\Lambda_n \leftarrow \Lambda_n \setminus \{\lambda\}, \Lambda_{\bar{n}} \leftarrow \Lambda_{\bar{n}} \cup \{\lambda\}$
15:     end if
16: end for
17: return $\Lambda_{\bar{n}}$
```

Granularity is the average size of the link sequences in $\Lambda_{\bar{n}}$. Smaller granularity indicates higher-quality results. The ideal is 1, which means that we can localize each observable neutrality violation to a single link.

False-positive rate: It is the fraction of neutral links that participate in neutral link sequences incorrectly present in $\Lambda_{\bar{n}}$. E.g., false-positive rate 10% means that 10% of the neutral links participate in a neutral link sequence that is incorrectly in $\Lambda_{\bar{n}}$.

The core of our algorithm is Algorithm 1, which identifies all the non-neutral link sequences that are identifiable:

- Lines 1–12: We add to set Λ_n every link sequence λ for which Π_λ contains at least 2 path pairs (which is equivalent to at least 5 pathsets).

- Lines 13–16: We move to set $\Lambda_{\bar{n}}$ any link sequence $\lambda \in \Lambda_n$ for which System 4 has no solution.

If we assume no measurement errors, Algorithm 1 suffers 0 false-positives and potentially a few false-negatives corresponding to the non-identifiable non-neutral link sequences. This is because its output consists exactly of all the identifiable non-neutral link sequences: (a) Every link sequence $\lambda \in \Lambda_{\bar{n}}$ is non-neutral. We have picked only link sequences for which System 4 does not have a solution. According to Lemma 2, any such link sequence is non-neutral. (b) Every non-neutral link sequence $\lambda \notin \Lambda_{\bar{n}}$ is non-identifiable. We have discarded only link sequences for which System 4 does have a solution. By Definition 2, any such link sequence is non-identifiable.

For example, consider the network in Figure 5(a), and suppose both links l_1 and l_2 are non-neutral. In this case, there are two non-neutral link sequences that are identifiable ($\langle l_1 \rangle, \langle l_1, l_2 \rangle$) and one non-neutral link sequence that is not ($\langle l_2 \rangle$). The algorithm correctly identifies the former: At line 8, $\Lambda_n = \{\langle l_1 \rangle, \langle l_1, l_2 \rangle\}$. Link sequence $\langle l_2 \rangle$ has not been added to Λ_n, because there exists no path pair such that $Links(p_i) \cap Links(p_j) = \{l_2\}$. At line 16, $\Lambda_{\bar{n}} = \{\langle l_1 \rangle, \langle l_1, l_2 \rangle\}$, because both $\langle l_1 \rangle$ and $\langle l_1, l_2 \rangle$ allow the formation of an unsolvable System 4. Hence, in this example, the algorithm's false-negative rate is 0 (both non-neutral links are present in $\Lambda_{\bar{n}}$) and the false-positive rate is also 0. The granularity is 1.5 (the average length of the identified non-neutral link sequences), which reflects our uncertainty about the neutrality of link l_2.

After running Algorithm 1, we remove from $\Lambda_{\bar{n}}$ all redundant link sequences. For example, suppose we have: $\Lambda_{\bar{n}} = \{\langle l_1, l_2 \rangle, \langle l_2, l_3 \rangle, \langle l_1, l_2, l_3 \rangle\}$; in this case, $\langle l_1, l_2, l_3 \rangle$ is redundant, because its presence in $\Lambda_{\bar{n}}$ does not add new information about the neutrality of the network. Formally, we consider a link sequence $\lambda \in \Lambda_{\bar{n}}$ *redundant*, if and only if:

$$\begin{aligned} \exists \{\lambda_i | i = 1..m\} \ &: \lambda_i \in \Lambda_n \cup \Lambda_{\bar{n}},\ \forall i \in [1, m] \\ \exists i \in [1, m] \ &: \ \lambda_i \in \Lambda_{\bar{n}} \\ \cup_{i=1}^{m} \lambda_i &= \lambda. \end{aligned}$$

In words, there exists a set of link sequences $\{\lambda_i\}$ such that: all of them are either in Λ_n or $\Lambda_{\bar{n}}$, at least one of them is in $\Lambda_{\bar{n}}$ (has been identified as non-neutral), and their union is equal to λ.

6. EXPERIMENTAL EVALUATION

In this section, we first describe our network emulator (Section 6.1) and how we process the measurements that we collect from it (Section 6.2). Then we present experimental results from two small topologies (Sections 6.3 and 6.4) and close with take-away points (Section 6.5).

6.1 Network Emulator

We perform our experiments within an open-source network emulator, where end-hosts generate actual TCP traffic and network links implement actual traffic-differentiation mechanisms. We do not simulate packet loss or queuing delay: traffic experiences actual packet loss and queuing delay depending on the queuing policies and the level of congestion it encounters in the network. We do not assume noise-free end-to-end measurements: end-hosts measure the performance of end-to-end paths based on the actual traffic they exchange.

Our emulator is similar to ModelNet [29], with the difference that the network is emulated by a user-level process, not a kernel module. We opted for a user-level implementation, because we found it easier to debug, and it avoids the overhead of porting between different operating systems. As in ModelNet, the role of end-hosts is played by virtual network interfaces that exchange real traffic. The role of the network (the relays) is played by a *network process* that implements network queues and policies. The size of each queue is set according to the maximum round-trip time (RTT) experienced by traffic traversing the queue. The only aspect of the network that is simulated is the propagation delay of links.

We implemented two traffic-differentiation mechanisms that are deployed in current network devices: policing and shaping. Both of them limit the fraction of a link's capacity that is consumed by a given performance class. Policing relies on a token bucket; the rate at which tokens are added to the bucket determines the maximum rate of the targeted performance class; the size of the bucket determines the maximum allowed burst; any excess traffic (that does not fit in the bucket) is immediately dropped. Shaping is similar, with the difference that any excess traffic is buffered in a dedicated queue.

In the experiments presented in this paper, the network either is neutral or implements $|C| = 2$ performance classes. When we say that a network link "implements policing," we mean that it passes all class-2 traffic through one policer, whose rate varies across experiments from 50% to 20% of link capacity. When we say that a network link "implements shaping," we mean that it passes all class-2 traffic through one shaper, whose rate R varies across experiments from 50% to 20% of link capacity, while it passes all class-1 traffic through another shaper with rate $1-R$. Unless otherwise stated, link capacity and policing/shaping rate take the default values shown in Table 1.

In each experiment, the end-hosts generate TCP traffic for 10 minutes. Each pair of communicating end-hosts starts a number of parallel TCP flows with the transfer size following a Pareto distribution; when a TCP flow ends, a new one starts after an idle time that is governed by an exponential distribution. We chose this model, because there is evidence that it captures well the communication between pairs of Internet end-hosts [9], but it is not crucial to our results—it is just one way of generating dynamic traffic patterns. Across experiments, we vary the number of parallel flows per path, as well as the parameters of the Pareto and exponential distributions (that govern flow size and inter-flow idle time, respectively). Unless otherwise stated, these parameters take the default values shown in Table 1.

Parameter	Value(s)
Bottleneck capacity (Mbps)	100
RTT (ms)	**50**, 80, 120, 200
Policing/shaping rate (%)	20, **30**, 40, 50
Congestion-control algorithm	**CUBIC**, NewReno
Parallel TCP flows per path	1, 12, **15**, 20, 70
Mean TCP flow size (Mb)	1, **10**, 40, 10000
Mean inter-flow gap (s)	10
Loss threshold (%)	1, **5**, 10
Measurement interval (ms)	**100**, 200, 500

Table 1: Experiment parameters. Default values are in bold.

6.2 Measurement Processing

By our definition of neutrality, a neutral link l inflicts congestion on any path $p \in Paths(l)$ with the same probability. In practice, we found that this may not hold, because packet loss is not uniform: if path p_2 carries more and/or larger TCP flows than path p_1, the same neutral link l may drop a different fraction of packets from p_2 than p_1 during each time interval. As a result, even a neutral link may have different congestion probabilities for different performance classes.

To account for the above, we normalize our path measurements, such that they refer to traffic aggregates of the same rate. In particular, when we form System 4 for link sequence λ, we create the vector $\vec{y}$ as follows: (a) We discount certain packets from our measurements, such that: in each time interval, all paths in $Paths(\lambda)$ appear to have sent the same number of packets. (b) In each time interval, for each path $p \in Paths(\lambda)$, we count the fraction of packets that were lost; if this fraction is below a *loss threshold*, we decide that p was congestion-free in this interval. (c) In each time interval, for each pathset $\pi \in \Pi_\lambda$, we decide that π was congestion-free in this interval, when all its member paths were congestion-free. (d) We compute $\mathbb{P}(\pi)$ as the fraction of intervals in which π was congestion-free. The exact process by which we create $\vec{y}$ is stated as Algorithm 2 in our technical report [32].

A key step of our algorithm is to determine whether various instances of System 4 "have a solution" (line 13 of Algorithm 1). In practice, none of these systems has a perfect solution, but some are significantly "more unsolvable" than others. We decide whether System 4 for link sequence λ "has a solution" as follows: (a) We estimate λ's performance number based on each path pair in Π_λ. We compute the system's *unsolvability* as the absolute difference between the minimum and the maximum estimate. (b) Based on this unsolvability, we assign the system to one of two clusters using standard clustering; we decide that the system "has a solution," when it belongs to the low-unsolvability cluster.

6.3 Results for Single Shared Link

We first consider a Dumbbell topology with a single shared link that (in some experiments) implements traffic differentiation. This could correspond to the scenario in Figure 6(a), where an ISP throttles all traffic from servers S_3 and S_4. In this case, the topology in Figure 6(b) is the network slice that we need to monitor in order to reason about the neutrality of the shared link l_5.

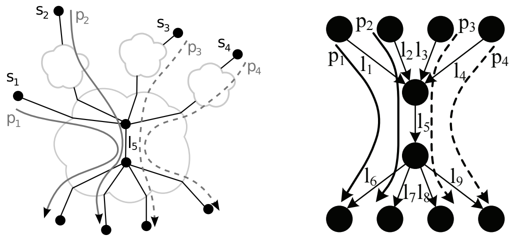

(a) Network. (b) Instantiated slice.

Figure 6: Experiment topology A. In some experiments, link l_5 polices traffic from paths p_3 and p_4.

Set	Link l_5 behavior	Varying parameter	Value(s)	
			c_1	c_2
1	Neutral	Mean flow size (Mb)	1	1, 10, 40, 10000
2	Neutral	RTT (ms)	50	50, 80, 120, 200
3	Neutral	Congestion control	CUBIC	CUBIC, NewReno
4	Policing	Mean flow size (Mb)	1, 10, 40, 10000	
5	Policing	RTT (ms)	50, 80, 120, 200	
6	Policing	Policing rate (%)	–	20, 30, 40, 50

Table 2: Experiment parameters for topology A.

Experimental setup.

We present six experiment sets, summarized in Table 2. We always refer to pathset $\{p_1, p_2\}$ as "class c_1" and to pathset $\{p_3, p_4\}$ as "class c_2." In experiments where the network is neutral, c_1 and c_2 do not constitute, strictly speaking, different performance classes, but we refer to them this way for simplicity.

In the first three experiment sets, the shared link does not implement any traffic differentiation. To make things difficult for our algorithm, we try to create network conditions that could be misinterpreted as non-neutrality. For instance, in experiment set #1, class c_1's average flow size is 1Mb, while class c_2's average flow size varies from 1Mb to 10Gb (a different value per experiment). Similarly, in sets #2 and #3, the two classes have different RTTs or use different congestion-control algorithms. As a result, in several of these experiments, the two classes exhibit dramatically different behavior, for instance, one class spends significantly more time in TCP slow start than the other.

In the last three experiment sets, the shared link polices the traffic in class c_2. Here, the difficult scenarios for our algorithm are the ones where all the paths carry the same kind of traffic. In each experiment set, we vary the average flow size, RTT, or policing rate of the shared link across experiments; however, in any single experiment, class-c_1 traffic and class-c_2 traffic have the same average flow size, RTT, and congestion-control algorithm.

In our technical report, we present three more experiment sets, where the shared link implements shaping. The results are similar to the ones of the policing experiments.

Results.

In all these experiments, our algorithm correctly decides whether the shared link is neutral or not.

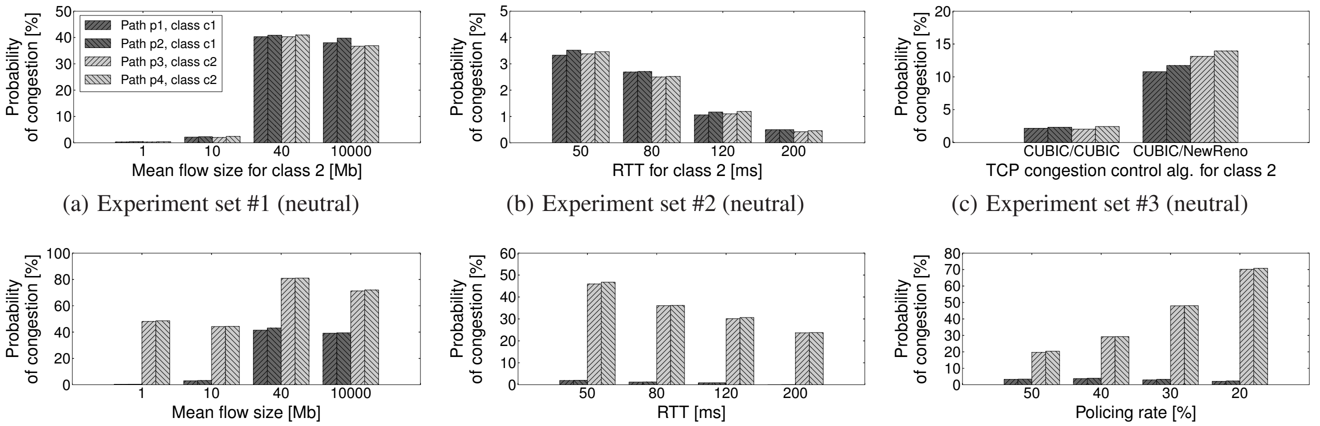

(a) Experiment set #1 (neutral)

(b) Experiment set #2 (neutral)

(c) Experiment set #3 (neutral)

(d) Experiment set #4 (policing)

(e) Experiment set #5 (policing)

(f) Experiment set #6 (policing)

Figure 7: External observations for neutral and non-neutral network, topology A. Parameters in Table 2.

Figure 7 shows the external observations for each experiment set. In each graph, the y-axis represents the probability that a path is congested, while the x-axis represents different experiments. For each x-axis value (each experiment), there are four data points, one for each of the four paths in our topology. For instance, in experiment set #1, when class c_2 has mean flow size 40Mb, each of the four paths is congested with probability 40% (Figure 7(a), third set of bars).

Figure 7 provides insight into how the algorithm works: When the shared link does not implement traffic differentiation, the 4 paths are congested with the same probability (top three graphs in Figure 7), which leads to consistent observations. When the shared link implements policing, the two paths in class c_2 are congested significantly more often than the two paths in class c_1 (bottom three graphs in Figure 7), which leads to inconsistent observations.

6.4 Results for Multiple Shared Links

Next, we consider the topology in Figure 8, which has multiple shared links. Links l_5, l_{14}, and l_{20} implement policing, while the other links do not implement explicit traffic differentiation. This could correspond to the scenario where routers R_1 to R_5 form the backbone of a tier-1 ISP, while each of routers R_6, R_7, R_{10}, R_{11}, and R_{12} belongs to a different tier-2 ISP or content provider. The tier-1 ISP uses policing on links l_{14} and l_{20} to throttle video or P2P traffic entering its network from routers R_7 and R_{11}, respectively; it uses policing on link l_5 to prevent internal P2P traffic from overloading its backbone network. We do not intend this to be a realistic topology, but to create a challenging scenario for our algorithm, with multiple shared links and bottlenecks.

Experimental setup.

We present an experiment where the network differentiates against long flows. There are three types of end-hosts: dark gray end-hosts with lines exchange short flows, light gray end-hosts with lines exchange long flows that are policed by links l_5, l_{14}, and l_{20} (this is the class-c_2 traffic), and white end-hosts exchange a mix of short and long flows, but they do not participate in the measurements (they provide background traffic). Table 3 shows the exact parameters for each type.

Results.

In this experiment, our algorithm suffers no false-positives and no false-negatives (each of the three policing links appears in at least one link sequence that is classified as non-neutral). It achieves granularity 2.7.

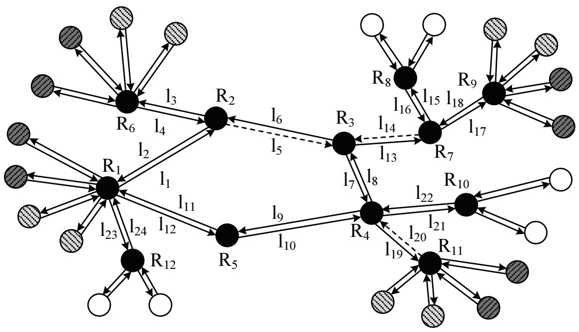

Figure 8: Experiment topology B. Dark gray end-hosts with lines exchange short flows. Light gray end-hosts with lines exchange long flows, which are policed by links l_5, l_{14}, and l_{20}. White end-hosts exchange a mix of short and long flows, but do not participate in the measurements.

End-host group	Number and size of parallel TCP flows per path
Dark gray	$1 \times$ 1Mb $+1 \times$ 10Mb $+1 \times$ 40Mb
Light gray	$1 \times$ 10Gb
White	$1 \times$ 1Mb $+1 \times$ 10Mb $+1 \times$ 40Mb $+1 \times$ 10Gb

Table 3: Traffic characteristics for topology B.

Figure 9(a) summarizes the actual performance of each link with respect to each path. These numbers are ground truth, directly measured by the network; our algorithm does not use them in any way. For each link, we show two boxplots: the left one summarizes the link's actual performance for class c_1, and the right one summarizes its actual performance for class c_2. To create each boxplot, we measure the performance of the link with respect to every individual path traversing the link. For instance, consider link l_{20}: according to the figure, this link never introduces congestion into class-c_1 paths (left boxplot), while it introduces congestion on average 4% of the time into class-c_2 paths (right boxplot).

We see that, for links l_5, l_{14}, and l_{20}, the two boxplots are significantly further apart than for the rest of the links. This validates the basic premise of our model: links implementing traffic differentiation have significantly higher performance-number variability than the rest of the links.

Figure 9(b) summarizes the performance of different link sequences as inferred by our algorithm. In this network, there are 28

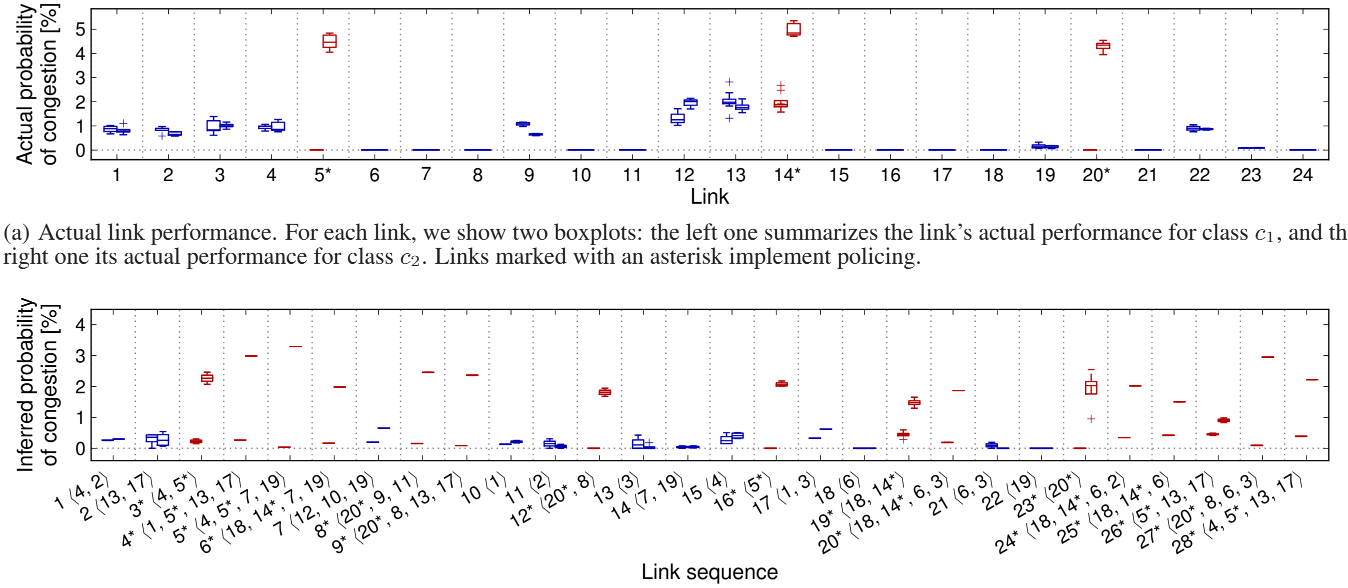

(a) Actual link performance. For each link, we show two boxplots: the left one summarizes the link's actual performance for class c_1, and the right one its actual performance for class c_2. Links marked with an asterisk implement policing.

(b) Inferred link-sequence performance. For each link sequence, we show two boxplots: the left one summarizes its inferred performance for class c_1, and the right one its inferred performance for class c_2. Link sequences marked with an asterisk include at least one policing link.

Figure 9: Ground truth and algorithm results for topology B. Parameters in Table 3.

link sequences with two or more path pairs in Π_λ, 16 of them non-neutral and identifiable. For each such link sequence λ, we show two boxplots: the left one summarizes λ's inferred performance for class c_1, and the right one summarizes its inferred performance for class c_2. To create each boxplot, we infer λ's performance based on different path pairs (different subsets of equations of System 4). For instance, consider link sequence #28 $= \langle l_4, l_5, l_{13}, l_{17} \rangle$: according to the figure, if we monitor only path pairs in class c_1, we infer that this link sequence almost never introduces congestion (left boxplot); if we monitor only path pairs in class c_2, we infer that the same link sequence introduces congestion on average 2% of the time (right boxplot).

We see that, for the link sequences that include link l_5, l_{14}, or l_{20}, the two boxplots are significantly further apart than for the rest. This validates the basic premise of our algorithm: links implementing traffic differentiation result in significantly more inconsistent external observations than the rest of the links.

Our algorithm suffers no false-negatives in this experiment, even though it incorrectly classifies non-neutral link sequences #19, #25, and #26 as neutral. These three link sequences do introduce different levels of congestion into the two performance classes, however, the difference is small enough to confuse the clustering algorithm. In this particular experiment, these mistakes do not result in false-negatives, but they do worsen granularity. For instance, link sequence #19 $= \langle l_{18}, l_{14} \rangle$ is incorrectly classified as neutral. This does not lead to a false-negative, because non-neutral link l_{14} is included in link sequence #20 $= \langle l_{18}, l_{14}, l_6, l_3 \rangle$, which is correctly classified as non-neutral. However, it worsens the algorithm's granularity, because it causes long link sequence #20 to remain in $\Lambda_{\bar{n}}$ (whereas it would have been discarded as redundant, had #19 been correctly classified as non-neutral).

6.5 Conclusions

Our algorithm did not misclassify a neutral link sequence as non-neutral in any of our experiments, even when half the paths traversing that link carried 1Mb flows and the other half carried 10Gb flows. This is because our performance metric is robust to TCP dynamics: The performance number of a path indicates *how often* it suffers non-negligible packet loss, not *how much* packet loss it suffers. TCP dynamics may cause the same link to introduce different amounts of packet loss during the same time interval; however, when the link does not explicitly differentiate between the two paths, it is unlikely to introduce non-negligible packet loss in one path and not in the other during the same time interval.

Congestion did not interfere with neutrality inference in any of our experiments. In the experiment on topology B, there exist both neutral and non-neutral, severely congested links. For instance, both links l_{13} and l_{14} operate close to capacity; if we look at packet loss and queue occupancy for these two links over time (shown in our technical report), there is no clue that l_{14} applies traffic differentiation while l_{13} does not. This does not affect the algorithm, because congestion on its own does not lead to significantly inconsistent external observations; only congestion that is preferentially inflicted on some paths does.

A key difference from network tomography is that we neither target nor require accurate inference of the performance of link sequences. For example, link l_{20} has actual congestion probabilities 0 and 4% for the two classes (Figure 9(a)), whereas our algorithm infers that it has congestion probabilities 0 and 2% (Figure 9(b), link sequence #23). This is because the algorithm infers the link's congestion probabilities for normalized traffic aggregates (Section 6.2), which are conservative estimates of the link's congestion probabilities for the two performance classes. Despite this, our algorithm correctly classifies the link as non-neutral, because it uses clustering: a link sequence λ is classified as non-neutral as long as its inferred performance numbers (in this case 0 and 2%) are sufficiently different that λ is assigned to the high-unsolvability cluster (Section 6.2).

As a side-note, we found that modern TCP variants are designed to converge with minimal packet loss. This is detrimental to tomography algorithms that rely on packet-loss measurements, e.g., to identify bottleneck links. Our performance metric is robust to such cautious congestion control, because—as mentioned above—it is a function of the frequency, not severity of loss events. Cautious congestion control may enable all classes to converge with minimal packet loss; however, when a link implements traffic differentiation, it necessarily introduces more loss events into deprioritized traffic than the rest, even if each of these events is not severe.

We close by noting that we repeated our experiments with all the loss thresholds and measurement intervals stated in Table 1, and there was no significant change in the results.

7. DISCUSSION

In this section, we discuss open issues. We further discuss how to relax Assumptions #2 and #3 (Section 2.2) in our technical report [32].

Measurement platform.

We assume the existence of a measurement platform and knowledge of the network graph that interconnects the measurement points. The most realistic deployment option is to use an existing platform where coalitions of end-hosts periodically measure the performance of the paths between them and upload the results to a centralized location for processing [4, 3, 24].

To discover the network topology, we can leverage existing work like Rocketfuel [27], AS-level traceroute [20], and manually collected ISP topologies [5]. Many of these proposals rely on IP traceroute, and one may ask: if we can use traceroute for discovering topology, why not use it also for measuring link or ISP performance (Section 1)? One reason is that a link can treat traceroute probes differently from other traffic (purposefully or not). That said, when we do deploy our algorithm, we will have to compare it against probe-based algorithms [19, 31].

Another challenge is collecting (performance and topology) measurements from sufficiently diverse vantage points: Today, the end-hosts that participate in measurement platforms are typically located in University or residential networks. By measuring the performance of the one-way paths between these end-hosts, one can detect neutrality violations against P2P traffic [15, 11] or against particular end-hosts. However, if we want to detect neutrality violations against a content provider, we also need to know the performance and topology of the one-way paths from this provider to various end-hosts (which we cannot measure directly, assuming the provider does not participate in the measurement platform). One option we are exploring is to infer the performance of one-way paths from round-trip performance based on TCP semantics [25], and to infer the topology of the one-way paths using reverse traceroute [17].

Path versus flow differentiation.

We define a non-neutral link as one that differentiates between traffic from different paths, as opposed to one that differentiates by traffic type (which is the typical definition). What happens when the network does differentiate by traffic type, e.g., throttles BitTorrent traffic?

In a realistic scenario, we expect our algorithm to detect differentiation by traffic type without requiring any changes. Consider a scenario where each path carries a mix of traffic types, but different paths carry different mixes. For instance, any path from a content provider to an end-host carries only non-BitTorrent traffic, whereas any path between two end-hosts carries both BitTorrent and non-BitTorrent traffic. In this case, any link that differentiates against BitTorrent traffic also differentiates against paths that carry BitTorrent traffic (e.g., it drops packets from the these paths more often than from the rest); hence, differentiation by type results in differentiation by path, which is what our algorithm detects.

In the worst-case scenario, each path carries roughly the same mix of traffic types. To deal with this case, we need to redefine a non-neutral link as one that differentiates not between different paths, but between different traffic aggregates (where each traffic aggregate follows the same path, but there may be multiple traffic aggregates per path). This change of definition affects only the way we collect our external observations: in System 3, each element of the vector $\vec{y}$ corresponds to a different set of traffic aggregates (as opposed to a different pathset). We can create traffic aggregates as follows: for each path, we measure the end-to-end performance experienced by each UDP or TCP flow, and we classify flows that experience the same performance in every time interval into the same traffic aggregate.

Performance metrics.

We restrict ourselves to additive performance metrics that can be defined not only for paths, but also for pathsets. What happens when the network violates neutrality, but that results in inconsistent latency or jitter—in general, performance metrics that cannot be defined for pathsets?

A promising approach is to convert our desired performance metric into one that *can* be defined for pathsets. For instance, if we want to detect neutrality violations that result in inconsistent latency, we can define a link's performance as the probability that the link introduces latency below some pre-configured threshold; then we can define a pathset's performance as the probability that all the links traversed by the pathset introduce latency below some pre-configured threshold.

Defining performance as a probability of a congestion event means that our external observations are measurements of the frequency with which paths and pathsets are congested. The limitation of our approach is that we cannot detect a neutrality violation if it lasts for one (in practice, a small number of) measurement interval(s). However, our detection is not probabilistic: as long as a neutrality violation lasts for a significant number of intervals (and it is externally observable), our approach can detect it.

8. RELATED WORK

Several proposals detect traffic differentiation based on transport-layer headers or payload [18, 31, 15, 11]. The common theme of these proposals is to have two end-hosts exchange two different traffic flows (e.g., a BitTorrent flow and a flow that contains random bytes) over the same network path; if the treatment of the two flows is significantly different, then the network path between end-user and monitoring server must be non-neutral. Unlike our algorithms, these systems were not designed to detect traffic differentiation that affects all flows of an end-host, nor localize it to specific links.

NetPolice [31] belongs to the above body of work, but moreover detects whether an ISP treats traffic differently based on routing information, e.g., previous- or next-hop AS. The main idea is to use traceroute-like probes to measure the loss rate inflicted by an ISP on traffic associated with different neighboring ASes; if these loss rates are significantly different from each other, then the ISP must be non-neutral. We focus, instead, on the scenario where we cannot rely on traceroute-like probes (or any other mechanism) to directly measure the loss rates of links or link sequences (e.g., because there is no practical way of generating such probes, or probes are not treated the same as other traffic).

Nano [28] "detects whether an ISP causes performance degradation for a service when compared to performance for the same service through other ISPs." We view this work and ours as complementary: it detects whether two different ISPs inflict different performance on the same kind of traffic; we detect whether any particular link (or link sequence) inflicts different performance on different traffic.

ShaperProbe [16] and Packsen [30] detect whether a network path is shaping an end-user's traffic and also determine the parameters of the shaper. The main idea is to have the end-user send traffic to a monitoring server, while keeping track of the rate at which the server receives the user's traffic; the evolution of the receiving rate can reveal the presence of a shaper between end-user and server, as well as the shaper's properties. We view this work and ours as complementary: it detects whether any single flow is subjected to shaping and identifies the parameters of the shaper; we detect whether different traffic flows are subjected to different treatment (of any kind) and localize this differentiation to specific links.

9. CONCLUSION

We studied the problem of detecting network-neutrality violations and localizing them to specific links. We presented conditions under which neutrality violations are observable and non-neutral links are identifiable based solely on external observations. Based on our analysis, we proposed an algorithm that takes as input a network graph and end-to-end measurements, and it identifies non-neutral link sequences; we evaluated it using network emulation. Our results indicate that it is indeed possible to reason about network neutrality, even when we know nothing about the internal behavior of the network. We hope that this work is a small step toward making the Internet more transparent.

Acknowledgments. We would like to thank Constantine Dovrolis for encouraging us to pursue this work despite early difficulties; Udi Weinsberg, our shepherd Aditya Akella, and the 6 anonymous SIGCOMM reviewers, for their deep, thorough reviews; and Mihai Dobrescu, Jonas Fietz, Dimitri Melissovas, Pavlos Nikolopoulos, Patrick Thiran, for helping us improve the paper. This work was supported by the Swiss National Science Foundation (SNSF).

10. REFERENCES

[1] Is my ISP Throttling YouTube? http://productforums.google.com/forum/#!topic/youtube/fUig1oN9ce4.

[2] LINE Network Emulator. http://wiki.epfl.ch/line/.

[3] Measurement Lab. http://www.measurementlab.net/.

[4] PlanetLab: An Open Platform for Developing, Deploying, and Accessing Planetary-scale Services. http://www.planet-lab.org/.

[5] The Internet Topology Zoo. http://www.topology-zoo.org/.

[6] T. Bu, N. Duffield, F. L. Presti, and D. Towsley. Network Tomography on General Topologies. In *Proceedings of the ACM SIGMETRICS Conference*, 2002.

[7] R. Caceres, N. G. Duffield, J. Horowitz, and D. Towsley. Multicast-based Inference of Network-Internal Loss Characteristics. *IEEE Transactions on Information Theory*, 45:2462–2480, 1999.

[8] M. Coates and R. Nowak. Network Loss Inference Using Unicast End-to-End Measurement. In *Proceedings of the ITC Specialist Seminar on IP Traffic Measurement, Modeling and Management*, 2000.

[9] M. E. Crovella and A. Bestavros. Self-Similarity in World Wide Web Traffic: Evidence and Possible Causes. *IEEE/ACM Transactions on Networking*, 5(6):835–846, December 1997.

[10] A. Dhamdhere, R. Teixeira, C. Drovolis, and C. Diot. NetDiagnoser: Troubleshooting Network Unreachabilities Using End-to-end Probes and Routing Data. In *Proceedings of the ACM CoNEXT Conference*, 2007.

[11] M. Dischinger, M. Marcon, S. Guha, K. P. Gummadi, R. Mahajan, and S. Saroiu. Glasnost: Enabling End Users to Detect Traffic Differentiation. In *Proceedings of the USENIX Symposium on Networked Systems Design and Implementation (NSDI)*, 2010.

[12] M. Dischinger, A. Mislove, A. Haeberlen, and K. P. Gummadi. Detecting BitTorrent Blocking. In *Proceedings of the ACM Internet Measurement Conference (IMC)*, 2008.

[13] N. G. Duffield. Network Tomography of Binary Network Performance Characteristics. *IEEE Transactions on Information Theory*, 52(12):5373–5388, December 2006.

[14] D. Ghita, K. Argyraki, and P. Thiran. Network Tomography on Correlated Links. In *Proceedings of the ACM Internet Measurement Conference (IMC)*, 2010.

[15] P. Kanuparthy and C. Dovrolis. DiffProbe: Detecting ISP Service Discrimination. In *Proceedings of the IEEE INFOCOM Conference*, 2010.

[16] P. Kanuparthy and C. Dovrolis. ShaperProbe: End-to-end Detection of ISP Traffic Shaping Using Active Methods. In *Proceedings of the ACM Internet Measurement Conference (IMC)*, 2011.

[17] E. Katz-Bassett, H. V. Madhyastha, V. K. Adhikari, C. Scott, J. Sherry, P. van Wesep, T. Anderson, and A. Krishnamurthy. Reverse Traceroute. In *Proceedings of the USENIX Symposium on Networked Systems Design and Implementation (NSDI)*, 2010.

[18] G. Lu, Y. Chen, S. Birrer, F. E. Bustamante, C. Y. Cheung, and X. Li. End-to-end Inference of Router Packet Forwarding Priority. In *Proceedings of the IEEE INFOCOM Conference*, 2007.

[19] R. Mahajan, N. Spring, D. Wetherall, and T. Anderson. User-level Internet Path Diagnosis. In *Proceedings of the ACM Symposium on Operating Systems Principles (SOSP)*, 2003.

[20] Z. M. Mao, J. Rexford, J. Wang, and R. H. Katz. Towards an Accurate AS-Level Traceroute Tool. In *Proceedings of the ACM SIGCOMM Conference*, 2003.

[21] H. X. Nguyen and P. Thiran. Network Loss Inference with Second Order Statistics of End-to-End Flows. In *Proceedings of the IEEE Internet Measurement Conference (IMC)*, 2007.

[22] H. X. Nguyen and P. Thiran. The Boolean Solution to the Congested IP Link Location Problem: Theory and Practice. In *Proceedings of the IEEE INFOCOM Conference*, 2007.

[23] V. N. Padmanabhan, L. Qiu, and H. J. Wang. Server-based Inference of Internet Performance. In *Proceedings of the IEEE INFOCOM Conference*, 2003.

[24] M. Sanchez, J. Otto, Z. Bischof, D. Choffnes, F. Bustamante, B. Krishnamurthy, and W. Williger. Dasu: Pushing Experiments to the Internet's Edge. In *Proceedings of the USENIX Symposium on Networked Systems Design and Implementation (NSDI)*, 2013.

[25] S. Savage. Sting: a TCP-based Network Measurement Tool. In *Proceedings of the USENIX Symposium on Internet Technologies and Systems (USITS)*, 1999.

[26] H. H. Song, L. Qiu, and Y. Zhang. NetQuest: A Flexible Framework for Large-Scale Network Measurement. In *Proceedings of the ACM SIGMETRICS Conference*, 2006.

[27] N. Spring, R. Mahajan, D. Wetherall, and T. Anderson. Measuring ISP topologies with Rocketfuel. *IEEE/ACM Transactions on Networking*, 12(1):2–16, February 2004.

[28] M. B. Tariq, M. Motiwala, N. Feamster, and M. Ammar. Detecting Network Neutrality Violations with Causal Inference. In *Proceedings of the ACM CoNEXT Conference*, 2008.

[29] A. Vahdat, K. Yocum, K. Walsh, P. Mahadevan, D. Kostic, J. Chase, and D. Becker. Scalability and Accuracy in a Large-Scale Network Emulator. In *Proceedings of the USENIX Symposium on Operating Systems Design and Implementation (OSDI)*, 2002.

[30] U. Weinsberg, A. Soule, and L. Massoulie. Inferring Traffic Shaping and Policy Parameters using End Host Measurements. In *Proceedings of the IEEE INFOCOM Mini-Conference*, 2011.

[31] Y. Zhang, Z. M. Mao, and M. Zhang. Detecting Traffic Differentiation in Backbone ISPs with NetPolice. In *Proceedings of the ACM Internet Measurement Conference (IMC)*, 2007.

[32] Z. Zhang, O. Mara, and K. Argyraki. Network Neutrality Inference. Technical report, École Polytechnique Fédérale de Lausanne, 2014. Available at http://infoscience.epfl.ch/record/186414.